Proceedings of the ASME 2009 International Design Engineering Technical Conferences & Computers and Information in Engineering Conference
IDETC/CIE 2009
August 30-September 2, 2009, San Diego, USA

DRAFT DETC2009-86841

ENERGY HARVESTING FROM VIBRATIONS WITH A NONLINEAR OSCILLATOR

David A.W. Barton
Engineering Mathematics
Queen's Building
University of Bristol
Bristol BS8 1TR, United Kingdom
Email: david.barton@bristol.ac.uk

Stephen G. Burrow
Aerospace Engineering
Queen's Building
University of Bristol
Bristol BS8 1TR, United Kingdom
Email: stephen.burrow@bristol.ac.uk

Lindsay R. Clare
Aerospace Engineering
Queen's Building
University of Bristol
Bristol BS8 1TR, United Kingdom
Email: aelrc@bristol.ac.uk

ABSTRACT

In this paper we present a nonlinear electromagnetic energy harvesting device that has a broadly resonant response. The nonlinearity is generated by a particular arrangement of magnets in conjunction with an iron-cored stator. We show the resonant response of the system to both pure-tone excitation and narrow-band random excitation. In addition to the primary resonance, the super-harmonic resonances of the harvester are also investigated and we show that the corresponding mechanical up-conversion of the excitation frequency may be useful for energy harvesting. The harvester is modeled using a Duffing-type equation and the results compared to the experimental data.

1 INTRODUCTION

Many existing vibration-powered energy harvesting devices are designed around the principle of linear resonance [1–5] where an inertial mass mounted on a spring-damper is excited at the resonant frequency of the spring. The benefits of this arrangement are clear: strong amplification of source vibrations and mechanically very simple. However, there are also numerous drawbacks, particularly when the geometry of the device is constrained in some way (for example when the maximum allowed displacement of the inertial mass is smaller than the excitation, as is the case when harvesting from human motion). One of the main limitations of a linear mass-spring-damper based energy harvester is that its resonant peak is very narrow [6, 7]. Thus, if the excitation frequency deviates from the resonant frequency of the harvester, very little power is generated. There have been several attempts to design tunable harvesters, either by changing the electrical loading [4] or by actively changing the mechanical properties of the system [8, 9]. However, these devices are in the early stages of development.

One area of research that has seen little progress until recently is the design of energy harvesters with nonlinear resonant behavior. Such devices offer the potential for broadband or multiple resonant responses allowing use in a wide variety of different environments. Initial work by Mann and Sims [10] has shown how nonlinear devices are more tolerant to manufacturing imperfections due to their higher bandwidth (making tuning less important). Triplett and Quinn [11] studied a weakly nonlinear model of a piezoelectric energy harvester and demonstrated that, in certain regimes, the nonlinear effect enhanced the performance of the device but, in other regimes, detracted from the performance. On the electrical side, nonlinear electrical coupling to a piezoelectric patch has been shown by Guyomar et al. [12] to improve power output significantly. In the related area of vibration absorption, nonlinear structures have been used much more extensively: Carrella et al. [13] use geometric nonlinearities to construct a spring with effectively zero linear stiffness to enable low-frequency vibration isolation; McFarland et al. [14] exploit the concept of *energy pumping* [15] (uni-directional energy transfer) to localize vibrational energy in a nonlinear attachment; also see the review article by Ibrahim [16] and references therein.

In this paper we investigate the behavior of a nonlinear energy harvester that has a broadband resonant response. The de-

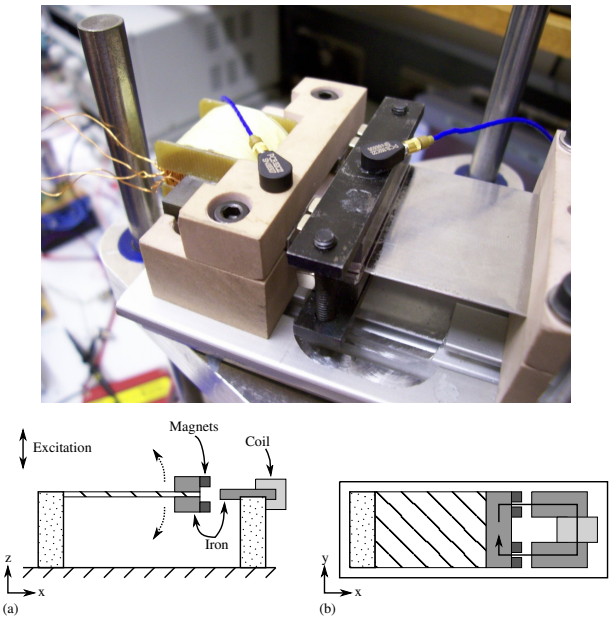

Figure 1. Top: a photograph of the harvester. Bottom: a schematic diagram of the harvester. The harvester consists of a cantilever beam with a tip-mass. The magnets on the tip are arranged such that there is a complete reversal of magnetic flux during one cycle.

vice uses electromagnetic transduction and uses materials that have a high magnetic permeability. The use of such materials results in strongly nonlinear mechanical characteristics, which is why they are typically avoided in electromagnetic energy harvester designs (which mostly use air-cored stators to ensure linear behavior). The use of high permeability materials enables far stronger coupling between the mechanical and electrical domains and, consequently, better energy extraction. In order to characterize the behavior of the harvester in 'real-world' situations we subject it to both pure sinusoidal excitation and narrow-band Gaussian white noise excitation with varying electrical loads. In reality, the excitation will be neither purely sinusoidal or purely random but, instead, somewhere between these two extremes.

The overview of the paper is as follows. In Sec. 2 the design of the nonlinear harvester is presented and discussed. Section 3 details the mathematical modeling of the harvester and its qualitative reduction to a Duffing-type equation. Experimental results are presented in Sec. 4: the effect on the frequency response of the harvester is shown for varying excitation strength and frequency and varying electrical loading. Furthermore, superharmonic resonances are investigated which shows that there is a strong possibility for using nonlinear devices to produce usable power levels at low frequencies. Conclusions are given in Sec. 5.

2 NONLINEAR HARVESTER DESIGN

Figure 1 shows a schematic diagram of the nonlinear energy harvester that is investigated in this paper. The harvester consists of a mass and a set of neodymium (NdFeB) magnets mounted at the tip of a cantilever beam in close proximity to a laminated iron stator. The magnets are arranged with alternating polarities in the (x, y)-plane such that a closed magnetic circuit exists with the magnetic flux passing through the stator (and coil) as illustrated in Fig. 1(b). The magnets are also arranged in the (x, z)-plane with alternating polarities to ensure that the flow of magnetic flux reverses direction as the beam vibrates. A voltage is generated across the coil in proportion to the rate of change of magnetic flux.

The use of a laminated iron-cored stator provides a high degree of coupling between the mechanical and electrical domains without the need for a large number of windings on the coil, unlike air-cored designs. Many electromagnetic energy harvesters in the literature use air-cored transducers to eliminate the extra damping caused by eddy currents and magnetic hysteresis, however, this results in poor coupling since air has a very low magnetic permeability. Furthermore, the air-cored designs may have greater electrical losses in their coils due to the increased coil length needed to obtain a usable output voltage. It is not yet clear which type of losses are more significant in energy harvester design.

While the use of iron in the energy harvester gives more optimal coupling, the interaction of the magnets with the iron stator also gives rise to large nonlinear effects in the mechanical domain. The magnetic forces effectively reduce the mechanical stiffness of the beam for small displacements. Thus, the overall effect is to create a hardening spring that has a lower natural frequency than the beam without the magnets attached. The reduction in the natural frequency is determined by the strength of the magnets and the size of the air gap between the magnets and the iron stator; if the air gap is decreased sufficiently, the device becomes bi-stable and the tip-mass will hop between between the two stable states when given a strong enough perturbation. Consequently, this design of energy harvester enables the resonant behavior of the device to be tuned significantly with only small mechanical changes.

If, when in the bistable regime, the stable states were equally favored (i.e., they lie in symmetric potential wells) it would be possible to make an energy harvester with almost zero linear stiffness by changing the air gap appropriately. This would be extremely useful for energy harvesting from very low frequency vibrations as well as enabling designs that incorporate more exotic ideas such as energy pumping [17]. Furthermore, in small scale designs, where it is not always possible to design a linear resonator with an appropriate natural frequency due to size constraints, this type of design could be successfully employed. However, due to the extreme sensitivity of the magnetic field to imperfections in the device, it is not possible to do this without

high-precision machining and placement of the magnetic parts. Consequently, zero stiffness can never be achieved in practice but it is possible to get close; in the experiments carried out on this device it was possible to reduce the first natural frequency of the beam from approximately 36Hz to approximately 17Hz by changing the size of the air gap without the aid of high-precision instruments.

For the experimental device investigated in this paper, we have focused on a parameter regime in which the device is monostable. Operating in the bistable regime does not appear to provide significant advantages, although the magnetic coupling (flux linkage) is stronger. A thorough investigation of the benefits of using a bistable energy harvester is currently in progress and is beyond the scope of the present paper. One significant consequence of the bistable configuration which we note here is that the motion of the tip mass may be chaotic if the excitation force is not sufficiently strong and this is not desirable for providing useful electrical output.

3 MATHEMATICAL MODELING

The mechanical part of the energy harvester as shown in Fig. 1 can be modeled as a cantilever beam using the Euler-Bernoulli equation with appropriate boundary conditions [18]. However, it is convenient to make the simplifying assumption that the beam is operating solely in its first mode. This is justified by the fact that the harvester is always excited at or below its first resonant frequency (approximately 24Hz in the experiments below) and the second resonant frequency is far higher (approximately 160Hz in the experiments below). Consequently, the mechanical part of the energy harvester is modeled as the mass-spring-damper system

$$m\ddot{u} + c_{\text{mech}}\dot{u} + k_{\text{mech}}u + F_{\text{mag}}(u,\dot{u}) = -m\ddot{v}$$

where F_{mag} is the magnetic interaction force and v is the displacement applied to the base of the energy harvester.

The magnetic part of the system is significantly more difficult to model due to the distributed nature of the fields involved. Consequently, as a first approximation, we assume the magnetic forces to be modeled well by a cubic polynomial in displacement and a linear function with respect to velocity:

$$F_{\text{mag}} := k_{\text{mag}}u + \beta_{\text{mag}}u^3 + c_{\text{mag}}\dot{u} + F_{\text{elec}}$$

where F_{elec} is the force reflected back from the electrical domain. The velocity term acts as an effective magnetic damping incorporating any losses due to the magnetic field's interaction with the iron-cored stator (e.g., eddy current losses and magnetic hysteresis). The coefficients of the polynomials are determined by fitting to experimental data; see Fig. 2. While this might seem a gross simplification of the physics, it provides a good approximation of the behavior of the energy harvester as shown by the experimental data. Furthermore, the alternative approaches, such as finite element electromagnetics, are very cumbersome and very few, if any, generally applicable design rules can be derived from them.

The bi-directional coupling between the magnetic and electrical domains occurs since a changing magnetic field strength (due to the change in position of the permanent magnets) will induce a potential difference across the coil. In turn, this potential difference will drive the flow of current around the electrical circuit and the flowing current will create a magnetic field in opposition to the original changes in the magnetic field.

The relationship between the position of the magnets/tip-mass and the magnetic field strength in the stator is approximately linear during normal operation as shown by Fig. 2. Consequently, there is a one-to-one relationship between the velocity of the magnets and the potential difference induced across the coil.

The final nonlinear model is derived by applying Kirchhoff's circuit equations to the simple electrical load of two resistors (one for the coil resistance and one for the load resistance) and an ideal voltage source in series. This gives

$$m\ddot{u} + (c_{\text{mech}} + c_{\text{mag}})\dot{u} + (k_{\text{mech}} + k_{\text{mag}})u + \beta_{\text{mag}}u^3 = -m\ddot{v} - \theta i,$$
$$\theta\dot{u} = Ri$$

where θ is a coupling coefficient and $R := R_{\text{coil}} + R_{\text{load}}$ is the total resistance in the electrical circuit. These two equations can be combined to give the Duffing-type equation

$$m\ddot{u} + (c_{\text{mech}} + c_{\text{mag}} + \theta^2/R)\dot{u} + (k_{\text{mech}} + k_{\text{mag}})u + \beta_{\text{mag}}u^3 = -m\ddot{v}. \quad (1)$$

The Duffing equation has been extensively studied in a wide variety of contexts and methods of solution can be found in any good textbook on nonlinear ordinary differential equations (see for example [19, 20]). For brevity, we omit the details here.

4 EXPERIMENTAL RESULTS

This section describes the experimental rig and the tests undertaken to investigate the dynamics of the nonlinear energy harvester. The tests were primarily frequency sweeps with either sinusoidal or narrow band noise as the excitation. Both the primary resonance and the super-harmonic resonances were considered.

When used in practice, it is unlikely that the energy harvester will experience either of the two extremes of excitation (that is, purely sinusoidal or purely random) and the "real" excitation will lie somewhere in the middle. For example, when harvesting energy from machine vibrations the excitation is likely to be well

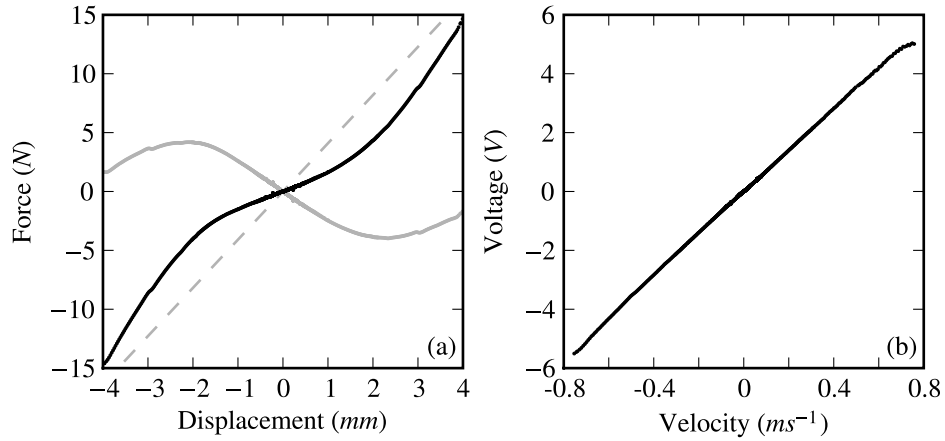

Figure 2. (a) Mechanical spring characteristics of the beam/magnet system. The solid gray curve and the dashed gray line show the magnetic and mechanical spring characteristics respectively; the solid black curve shows the overall spring characteristics. (b) Characteristics of the electromagnetic induction.

defined but have a significantly more complicated spectrum than just a simple sinusoid. Whereas, when harvesting from motion of people or animals the excitation will be much more random but still have some well defined characteristics. However, without a particular application in mind, these two extremes provide a guide to how the harvester will behave in reality.

4.1 Experimental set-up

Base excitation of the energy harvester was achieved using an electrodynamic shaker with a closed-loop position feedback controller to ensure reliable operation across all frequency ranges. Additionally, the shaker was orientated horizontally to ensure that no extra asymmetries were introduced into the system by the action of gravity. The energy harvester was instrumented with PCB Piezotronics accelerometers on its base and on the tip mass to provide positional measurements in addition to the voltage output of the coil.

When the harvester was excited with sinusoidal forcing, the position and velocity information was determined by numerically integrating the accelerometer output and determining the integration constants by the periodicity. Since the forcing frequency was relatively high, the drift of the accelerometer signal across one oscillation was negligible and so the position and velocity information obtained was reasonably accurate.

When the harvester was excited with narrow-band random forcing (and so the response was no longer periodic), the accelerometer data was first filtered to remove low frequency components (frequencies below 0.1Hz) before numerical integration. The resulting positional information had approximately a zero-mean suggesting that this was sufficient to remove the effects of accelerometer drift.

The narrow-band random signal was created by passing Gaussian white noise through a linear band-pass filter of the form

$$\ddot{f} + \gamma \dot{f} + \omega_f^2 f = \gamma^{\frac{1}{2}} \omega_f W \tag{2}$$

where ω_f is the center frequency, γ is the bandwidth of the filter and W is a Gaussian white noise source [21]. This was implemented in a dSpace real-time controller which also enabled automated testing of the harvester.

4.2 Physical characteristics

The system parameters of Eq. (1) where determined by performing an initial frequency sweep with the coil in an open circuit state. At a discrete set of frequencies the periodic motion of the harvester was recorded. By combining all these measurements is was possible to reconstruct the phase-space of Eq. (1) as a (position, velocity, acceleration) triplet and so measure the spring and damping characteristics; in the systems identification literature, this is known as the restoring force surface method [22].

Figure 2(a) shows the reconstructed force-displacement characteristic of the harvester for zero velocity. Over the region of operation shown, the force-displacement characteristic has a strong cubic element with minimal asymmetry. Consequently, the dynamics of the harvester are similar to that of a hardening spring. Figure 2(b) shows the reconstructed voltage-velocity characteristic of the harvester at *peak displacement*. This validates the assumption of a linear relationship between the velocity and voltage, which only starts to break at higher velocities.

The measured parameters for the model Eq. (1) are as follows: $m = 80\,\mathrm{g}$, $c_{\mathrm{mech}} = 0.06\,\mathrm{N\,s\,m^{-1}}$, $c_{\mathrm{mag}} = 0.24\,\mathrm{N\,s\,m^{-1}}$, $\theta = 7\,\mathrm{V\,s\,m^{-1}}$, $12\,\Omega \leq R \leq 212\Omega$, $k_{\mathrm{mech}} = 4.09 \times 10^3\,\mathrm{N\,m^{-1}}$, $k_{\mathrm{mag}} = -2.37 \times 10^3\,\mathrm{N\,m^{-1}}$, $\beta_{\mathrm{mag}} = 1.63 \times 10^8\,\mathrm{N\,m^{-3}}$.

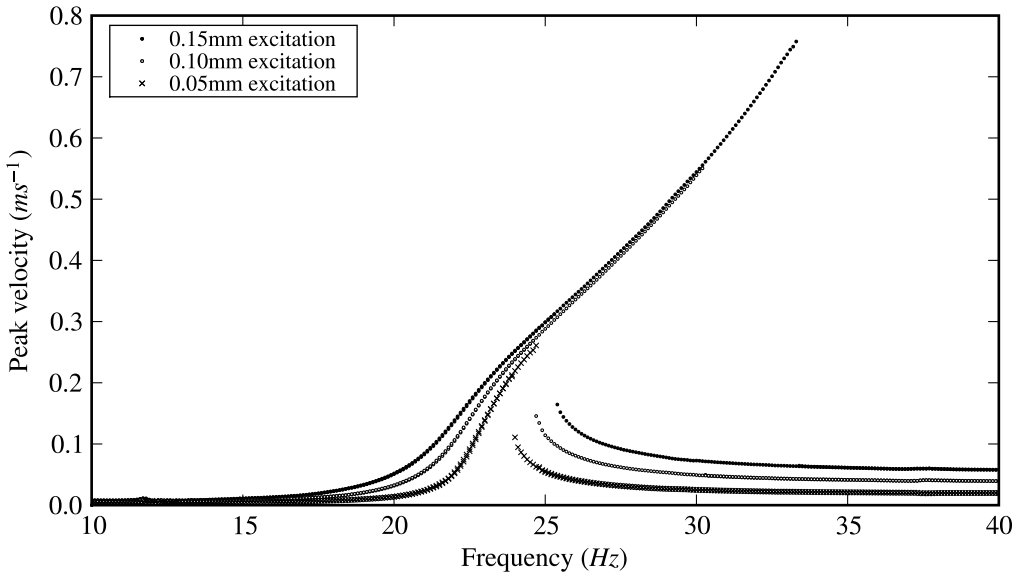

Figure 3. Experimental frequency sweeps (increasing frequency then decreasing frequency) for three amplitudes of excitation. The peak excitation displacement is kept constant across a frequency sweep using a closed-loop controller around the shaker.

4.3 Primary resonance — sinusoidal forcing

Figure 3 shows the fundamental behavior of the harvester as the excitation frequency varies. The velocity of the tip mass is plotted against frequency since this is the most important factor when considering the power output of the harvester. The forcing is a sinusoid with a fixed amplitude of displacement and the coil is in an open circuit state. Data is shown for three different forcing amplitudes: 0.1mm, 0.2mm and 0.3mm peak to peak displacement. The frequency is increased in steps of 0.2Hz from 10Hz to 40Hz and then decreased back to 10Hz to show the hysteresis in the response.

For small amplitude excitations, the harvester operates in a near-linear regime. There is a pronounced increase in the velocity near the linear resonance of 23.6Hz and little hysteresis in the response. For large amplitude excitations, the resonant behavior of the system is greatly increased and covers a wide band of frequencies, resulting in a large hysteresis loop where two stable states coexist (one high-energy state and one low-energy state).

Figure 4 presents a comparison of the experimental data and the model, which shows reasonable agreement between experiment and theory. The response of the model was computed using the numerical continuation software AUTO-97 [23] rather than the analytical formulas in [19, 20] due to the significant third harmonic component found in the response. The source of the discrepancies around the point of linear resonance are as yet unknown, but are likely to be due to the complicated damping mechanisms of magnetic hysteresis and eddy currents and the presence of small asymmetries in the harvester.

It is not surprising that the top branch of experimental results does not extend as far as the theory predicts. As the frequency of excitation is increased, the high-energy state becomes only weakly stable, its basin of attraction shrinks, and, consequently, small disturbances cause the harvester to be knocked into the low-energy state. With this in mind, we make the general comment that the resonant peaks of determined by nonlinear analysis of, for example, the Duffing equation should be treated with great care since the solution may only have a small basin of attraction which is not useful from a practical view point. However, it is relatively straightforward to determine the approximate size of the basin of attraction by numerical simulation.

Figure 5 shows the basins of attraction of the high-energy state (white) and the low-energy (black) for the model Eq. (1) when (a) $\omega = 27.5$Hz, (b) $\omega = 30$Hz, (c) $\omega = 32.5$Hz and (d) $\omega = 35$Hz. The basins are shown relative to the start of a period of forcing (i.e., the instantaneous forcing from the shaker is zero). It is immediately clear that the higher frequency, the more dominant the low-energy state becomes.

Figure 6(a) shows the peak velocity against frequency for six different electrical loading conditions. The electrical load is a variable resistor set to one of 50Ω, 75Ω, 100Ω, 150Ω, 200Ω or open circuit conditions. The experimental results show that there is little change in the peak velocity of the tip mass as the electrical damping is increased (equivalently, the resistive load is decreased). The primary difference in behavior comes from the change in drop down frequency. However, this jump up frequency remains constant with respect to the electrical loading. It should be noted that the voltage seen across the coil is not invariant with respect to the electrical damping since the relationship between velocity and voltage is also dependent on the electrical load.

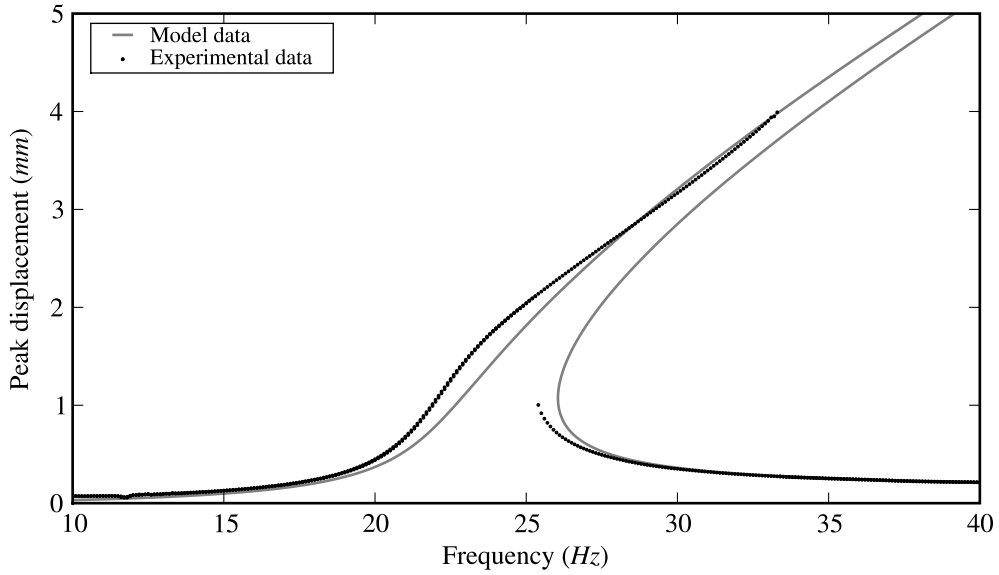

Figure 4. A comparison of the experimental frequency response and the model Eq. (1) frequency response. The discrepancies are likely to be due to un-modeled magnetic loss mechanisms.

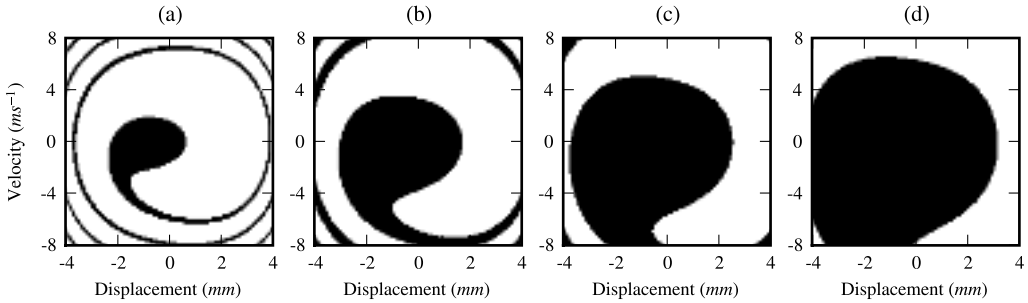

Figure 5. The basins of attraction of the model Eq. (1) computed by numerical simulation for (a) 27.5Hz, (b) 30Hz, (c) 32.5Hz, (d) 35Hz. The basin of attraction of the low energy state is colored in black and the basin of attraction of the high energy state is colored in white.

Figure 6(b) shows the peak electrical power developed in the load against frequency for same experiments. (Note: the open circuit condition results in zero power developed.) The optimum peak power condition occurs at approximately 100Ω, which is the same as the resistance required to achieve optimum peak power for a linear harvester with the same damping coefficients. When the resistance is decreased further, the peak power drops off. However, the power output at lower frequencies increases. Thus, at the edge of the bistable region (approximately 25Hz), the optimum peak power output is obtained for 50Ω.

These results provide further support for the notion that nonlinear energy harvesters can have wide-band responses. In effect, the bandwidth of the device can be increased considerably by including a variable load resistance into the electrical circuit design.

4.4 Primary resonance — random forcing

Figure 7 shows a comparison of the frequency response of the harvester in open circuit configuration with periodic excitation and narrow-band random excitation (bandwidth of 2Hz). The vertical axis shows the average tip velocity of the harvester, which is defined as the root-mean-square (RMS) velocity averaged over 10 seconds of excitation. Over the 10 second sampling window, the average RMS of the shaker displacement is approximately equal for both the periodic excitation and the random excitation.

The results in Fig. 7 show that the peak velocity attained by the harvester under periodic excitation is never reached by the harvester under random excitation. However, the harvester motion of the harvester does follow the high-energy branch briefly. The difference between the periodic and random excitation is due to the hopping between the different energy states as the random

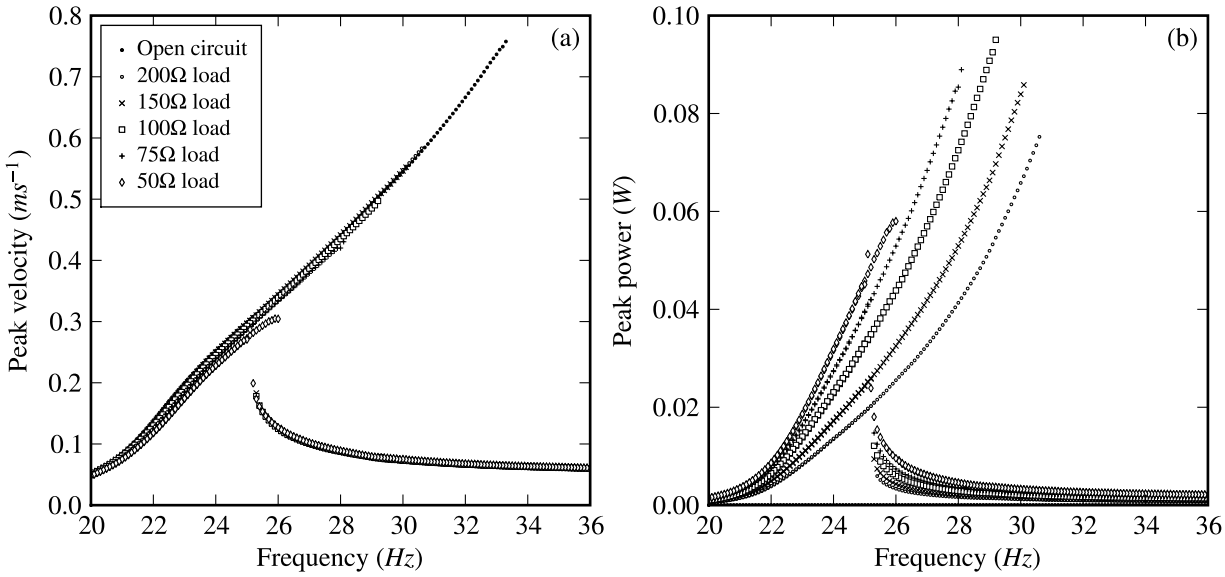

Figure 6. A comparison of frequency sweeps for varying electrical loads: (a) velocity, (b) power. Note: in the open circuit condition no power is developed.

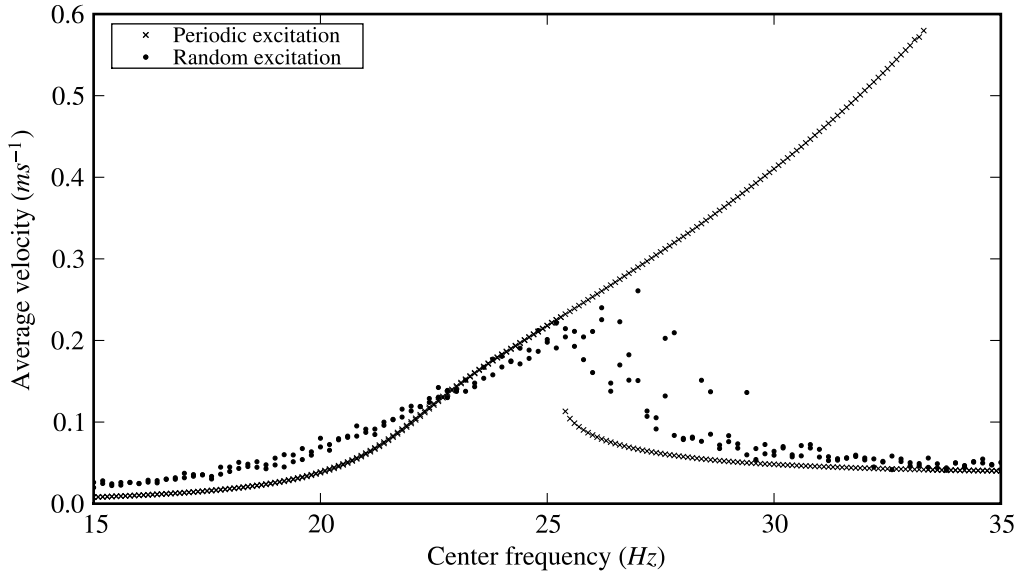

Figure 7. A comparison of the frequency response to a pure-tone excitation and a narrow-band random signal (2Hz bandwidth) of the energy harvester in open-circuit conditions. The response of the harvester to the random signal is averaged (RMS) over 10 seconds.

excitation changes in strength. For higher frequencies, once the high-energy state has been left the random excitation is not sufficiently strong to force the motion back into the high-energy state.

The effect of varying the bandwidth of the random excitation is shown in Fig. 8. The panels show the frequency responses for (a) 2Hz bandwidth, (b) 1Hz bandwidth, (c) 0.5Hz bandwidth and (d) 0.25Hz bandwidth. It could be argued that the jump up/down points in the frequency response are most clear in the narrowest bandwidth case, with the higher bandwidth cases smoothing out the distinction, but this is a tenuous conclusion based on the results shown here. Since there is not a great deal of difference between the results, this indicates that there is a very sharp transition at low bandwidth between the frequency response of the periodic excitation and the frequency responses shown here.

Further experiments (not shown) when varying the electrical loading indicate that the peak power output is obtained for very low electrical resistances (approximately 50Ω), which is consistent with the data presented in Fig. 6 since much of the high-

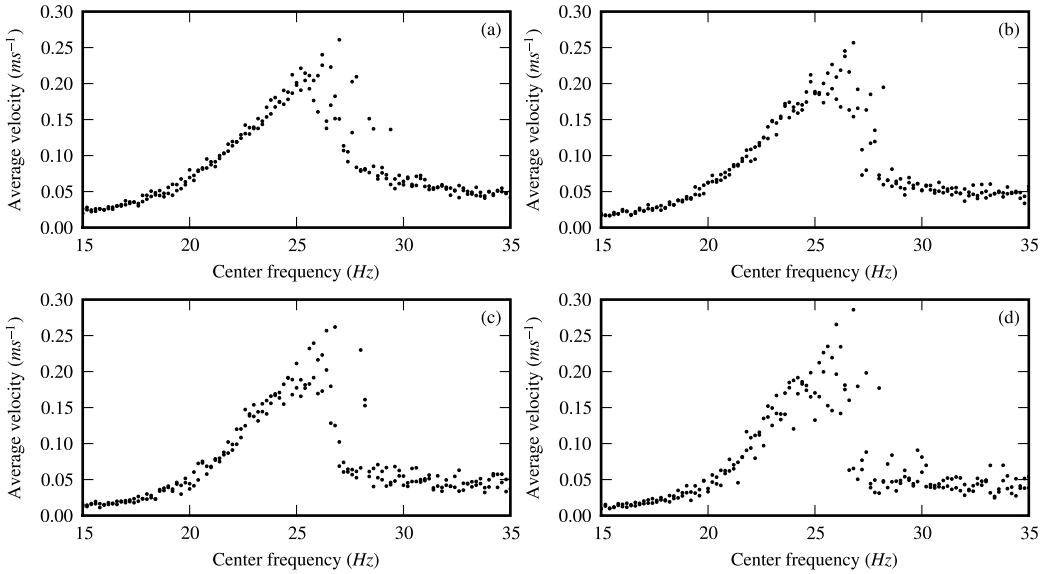

Figure 8. Frequency sweeps for varying bandwidth narrow-band random excitation. The corresponding bandwidths are (a) 2Hz, (b) 1Hz, (c) 0.5Hz, (d) 0.25Hz.

energy branch is not present.

Overall, the experimental results presented here are in broad agreement with theoretical findings on the Duffing equation with narrow-band excitation [21, 24]. Simply stated, increasing the bandwidth of the narrow-band excitation results in the device appearing increasingly linear — in effect the nonlinear behavior of the device is averaged out. If the bandwidth of the random excitation is decreased sufficiently (approximately 0.1Hz) most of the hysteresis loop seen in the pure-tone excitation case reappears.

4.5 Super-harmonics

Nonlinear devices often exhibit sub-/super-harmonic resonances, where the frequency of the response is lower/higher than the excitation frequency respectively. Of interest here are the super-harmonic responses, where the harvester responses at a higher frequency than the excitation frequency — a mechanical up-conversion of the frequency.

Figure 9 shows the low-frequency response of the nonlinear harvester for a variety of electrical loading conditions. Super-harmonic resonances at approximately 4.6Hz and 7.8Hz are clearly seen. The harvester is responding at its natural frequency when excited with a frequency of 5 times and 3 times lower respectively. These resonances are caused by the dominant cubic characteristic of the harvester. It is also possible to make out two additional super-harmonic resonances at 5.8Hz and 11.7Hz; these correspond to 1:4 resonances and 1:2 resonances respectively. These second two resonances are much smaller since they are determined by quadratic characteristics within the harvester (asymmetries in the force-displacement characteristics), which are very small.

The super-harmonic resonances appear very similar to linear resonances in that they possess no hysteretic regions in the frequency response. However, in general the super-harmonic resonances may also take the same form as the primary resonance if the nonlinear characteristics are suitably strong.

Although the super-harmonic response is far less than the primary response, the super-harmonic resonances may be useful in designing very low frequency energy harvesters or very small energy harvesters where it is not possible to build a linear resonator of sufficiently low frequency. In addition, the up-regulation of the frequency means that the overall displacement remains low while providing a relatively high velocity (compared with the excitation force). Consequently, future designs might seek to strengthen these super-harmonic resonances.

5 DISCUSSION AND CONCLUSIONS

In this paper we have shown that a nonlinear energy harvester is able to overcome some of the inherent limitations of a linear energy harvester, namely that of having a narrow resonant response. Moreover, the bandwidth of the harvester can be increased further with a varying resistive load. However, the advantages of the wide bandwidth are only apparent when there is a consistent (uninterrupted/non-random) vibration source (for example when the harvester is attached to a piece of rotating machinery) due to the coexistence of a low-energy state and a high-energy state. In particular, random excitations appear to average out the high-energy and low-energy states. We are currently investigating possible ways of incorporating a restarting mecha-

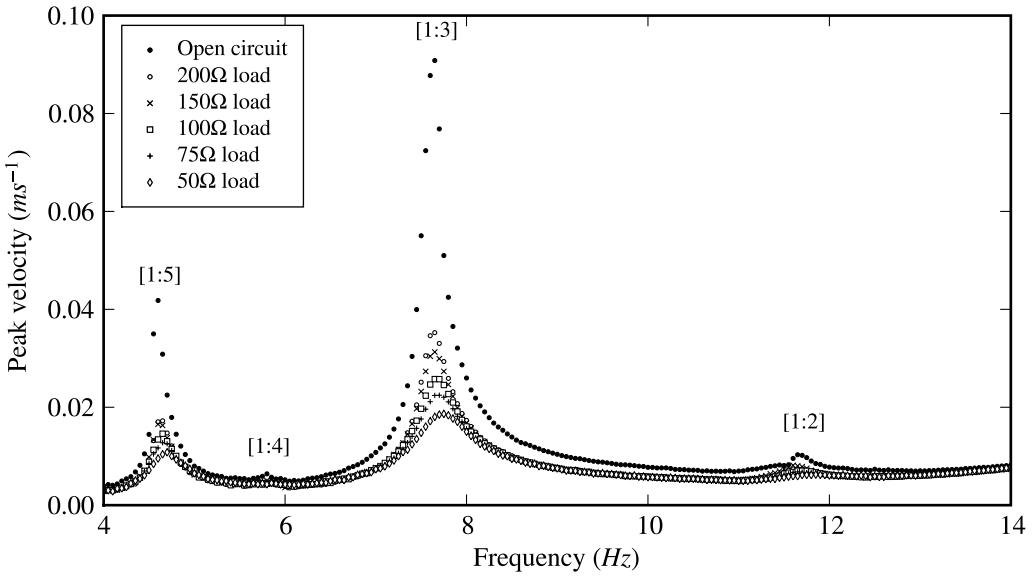

Figure 9. Super-harmonic resonances of the energy harvester for varying electrical loads. At the resonance peaks the harvester is responding at an integer multiple of the excitation frequency (as denoted above each peak in the figure). At the most prominent peak the harvester is responding at three times the excitation frequency.

nism, to over come sudden drops in the source vibration as found with random excitation, which uses a small amount of the previously harvested energy to perturb the harvester back into a high energy state.

While the model presented in this paper shows reasonable quantitative agreement with the experimental results, a much more in depth analysis of magnetic loss mechanisms is needed to fully model the system. A better model of the magnetic losses would also help determine the usefulness of iron-cored stator designs. The high magnetic permeability of iron gives a high degree of coupling between mechanical and electrical domains but it is still not clear if this benefit out weights the corresponding magnetic losses.

One important benefit of using a nonlinear harvester is the presence of super-harmonic resonances at frequencies well below the (linear) natural frequency. At these resonances the harvester responds at a higher frequency than the excitation frequency — a mechanical up-conversion of frequency. These super-harmonic resonances may enable the design of devices that resonate at low frequencies while still being able to extract moderate amounts of power.

ACKNOWLEDGMENTS

D.A.W.B. gratefully acknowledges the support of Great Western Research. S.G.B. and L.R.C. gratefully acknowledge the support of EPSRC grant EP/E044220/1 (Energy harvesting: vibration powered generators with non-linear compliance).

REFERENCES

[1] Williams, C., and Yates, R., 1996. "Analysis of a micro-electric generator for microsystems". *Sensors and Actuators A: Physical,* **52**(1–3), pp. 8–11.

[2] Williams, M., and Blakeborough, A., 2001. "Laboratory testing of structures under dynamic loads: an introductory review". *Philosophical Transactions of the Royal Society A,* **359**(1786), pp. 1651–1669.

[3] Baker, J., Roundy, S., and Wright, P., 2005. "Alternative geometries for increasing power density in vibration energy scavenging for wireless sensor networks". In Proceedings of 3rd International Energy Conversion Engineering Conference.

[4] Renno, J., Daqaq, M., and Inman, D., 2009. "On the optimal energy harvesting from a vibration source". *Journal of Sound and Vibration*. In press.

[5] Stephen, N., 2006. "On energy harvesting from ambient vibration". *Journal of Sound and Vibration,* **293**(1-2), May, pp. 409–425.

[6] Burrow, S., and Clare, L., 2007. "A resonant generator with non-linear compliance for energy harvesting in high vibrational environments". In Proceedings of Electric Machines & Drives Conference, IEMDC '07, Vol. 1, pp. 715–720.

[7] Burrow, S., Clare, L., Carrella, A., and Barton, D., 2008. "Vibration energy harvesters with non-linear compliance". In Proceedings of SPIE Smart Structures/NDE conference, pp. 692807–.

[8] Challa, V., Prasad, M., Shi, Y., and Fisher, F., 2008. "A vibration energy harvesting device with bidirectional reso-

nance frequency tunability". *Smart Materials and Structures,* **17**(1), pp. 015035–.

[9] Morris, D., Youngsman, J., Anderson, M., and Bahr, D., 2008. "A resonant frequency tunable, extensional mode piezoelectric vibration harvesting mechanism". *Smart Materials and Structures,* **17**(6), pp. 065021–.

[10] Mann, B., and Sims, N., 2009. "Energy harvesting from the nonlinear oscillations of magnetic levitation". *Journal of Sound and Vibration,* **319**(1–2), pp. 515–530.

[11] Triplett, A., and Quinn, D., 2008. The effect of nonlinear piezoelectric coupling on vibration-based energy harvesting. Preprint, Department of Mechanical Engineering, University of Akron.

[12] Guyomar, D., Badel, A., Lefeuvre, E., and Richard, C., 2005. "Toward energy harvesting using active materials and conversion improvement by nonlinear processing". *IEEE Transactions on Ultrasonics, Ferroelectrics and Frequency Control,* **52**(4), pp. 584–595.

[13] Carrella, A., Brennan, M., and Waters, T., 2007. "Static analysis of a passive vibration isolator with quasi-zero-stiffness characteristic". *Journal of Sound and Vibration,* **301**(3-5), pp. 678–689.

[14] McFarland, D. M., Bergman, L. A., and Vakakis, A. F., 2005. "Experimental study of non-linear energy pumping occurring at a single fast frequency". *International Journal of Non-Linear Mechanics,* **40**(6), pp. 891–899.

[15] Vakakis, A. F., and Gendelman, O., 2001. "Energy pumping in nonlinear mechanical oscillators: Part II—resonance capture". *Journal of Applied Mechanics,* **68**(1), pp. 42–48.

[16] Ibrahim, R., 2008. "Recent advances in nonlinear passive vibration isolators". *Journal of Sound and Vibration,* **314**(3-5), pp. 371–452.

[17] Quinn, D., Vakakis, A., and Bergman, L., 2007. "Vibration-based energy harvesting with essential nonlinearities". In Proceedings of the ASME IDETC. DETC2007-35457.

[18] Inman, D., 2007. *Engineering Vibration*. Prentice Hall.

[19] Jordan, D., and Smith, P., 1999. *Nonlinear ordinary differential equations*. Oxford University Press.

[20] Nayfeh, A., and Mook, D., 1995. *Nonlinear oscillations*. Wiley.

[21] Rajan, S., and Davies, H., 1988. "Multiple time scaling of the response of a Duffing oscillator to narrow-band random excitation". *Journal of Sound and Vibration,* **123**(3), pp. 497–506.

[22] Kerschen, G., Worden, K., Vakakis, A., and Golinval, J.-C., 2006. "Past, present and future of nonlinear system identification in structural dynamics". *Mechanical Systems and Signal Processing,* **20**(3), pp. 505–592.

[23] Doedel, E., Champneys, A., Fairgrieve, T., Kuznetsov, Y., Sandstede, B., and Wang, X., 1998. *AUTO 97: continuation and bifurcation software for ordinary differential equations*.

[24] Davies, H., and Rajan, S., 1988. "Random superharmonic and subharmonic response: Multiple time scaling of a Duffing oscillator". *Journal of Sound and Vibration,* **126**(2), pp. 195–208.